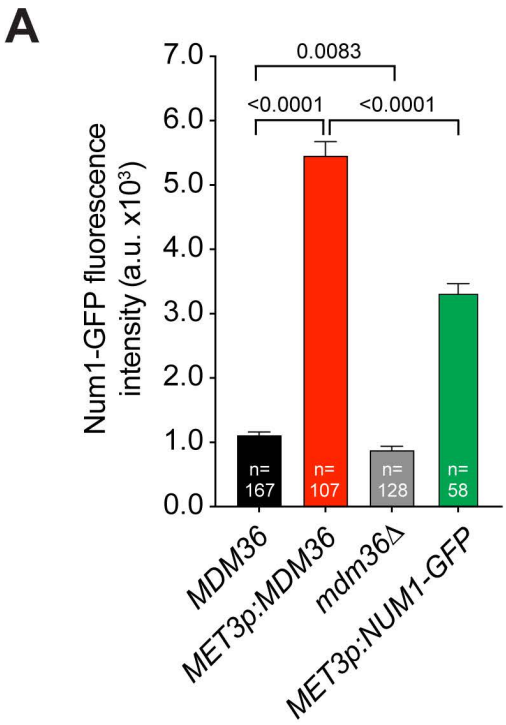

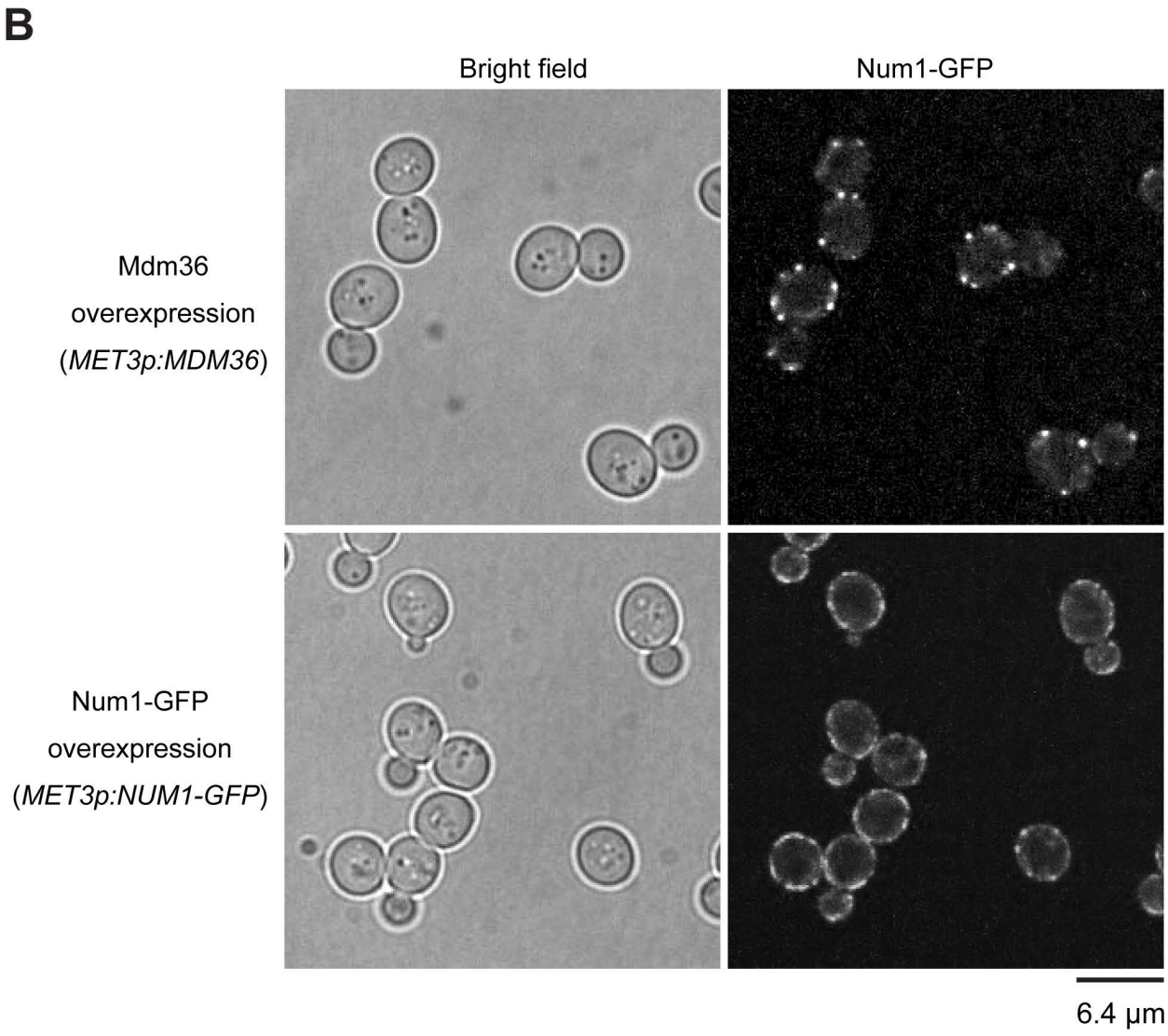

Journal of Cell Science • Supplementary information

Figure S1. Mdm36 promotes Num1 clustering. (A) Mean fluorescence intensity of individual Num1-GFP patches in indicated strains. Error bars represent SEM. *P*-value by unpaired *t* test. (B) Bright field and confocal images of cells overexpressing Mdm36 or Num1-GFP. Each confocal image is a maximum intensity projection of four optical sections spaced 0.2 μm apart from the equator of cells.

Journal of Cell Science • Supplementary information

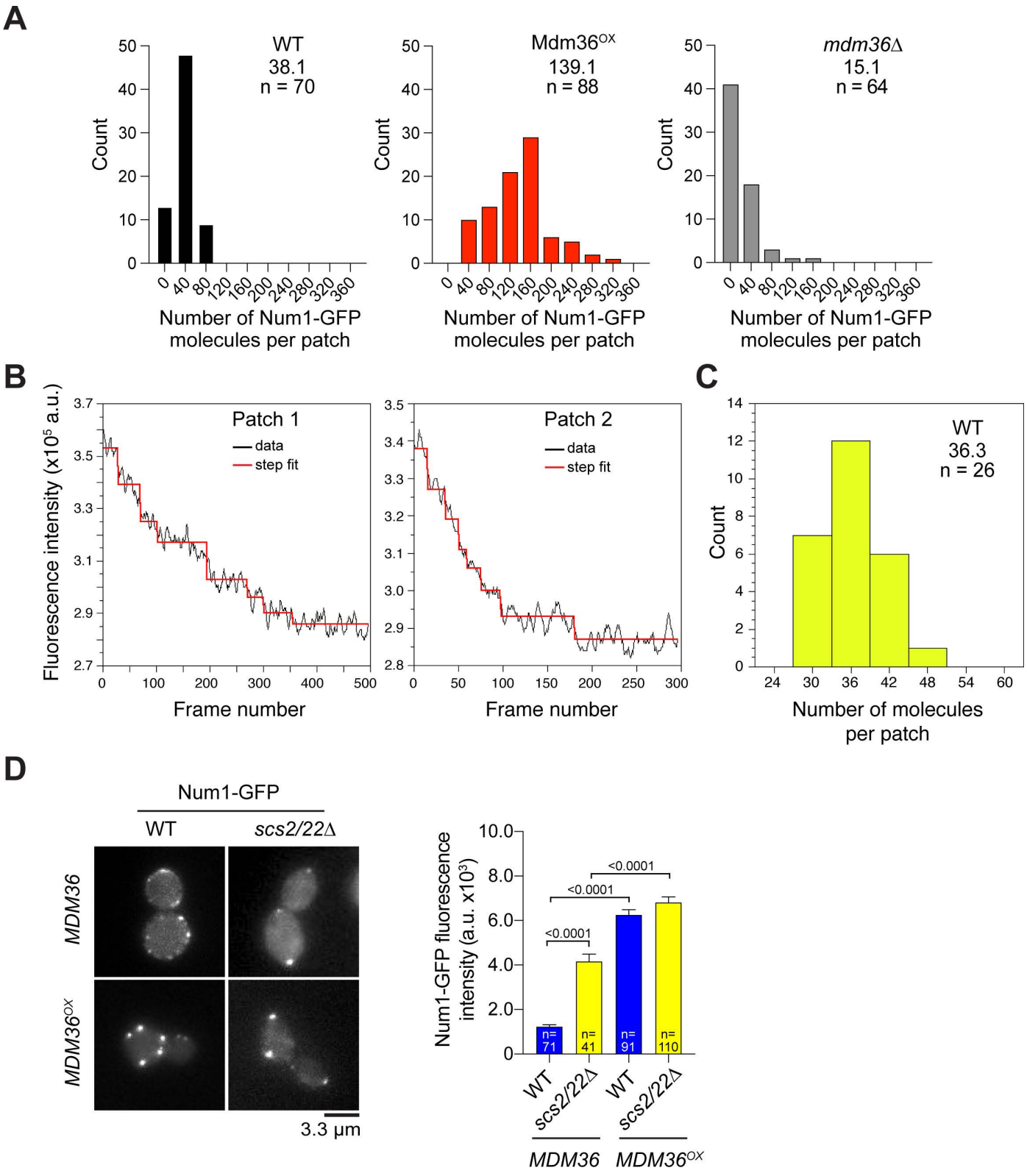

Journal of Cell Science • Supplementary information

Figure S2. Copy number of Num1-GFP molecules per cortical patch. (A) Histogram of protein copy number determined by ratiometric comparison to Mif2-GFP standard. Median copy number shown for each strain. (B) Representative data for bleaching step analysis. WT cells expressing Num1-GFP were imaged continuously in a single focal plane with a 250-ms exposure for each frame. Intensities of individual Num1-GFP patches were quantified over the course of the fluorescence decay, filtered by a five-frame rolling average, and analyzed by STEPFINDER to detect bleaching steps. Plots show filtered intensity traces (black) along with step fits obtained from STEPFINDER (red). (C) Histogram of protein copy number estimated by bleaching step analysis. Median copy number per cortical patch for Num1-GFP in WT cells is shown. **Num1 redistributes to bud tip and mother apex in Mdm36^{ox} cells lacking Scs2 and Scs22.** (D) Wide-field images of Num1-GFP in WT and *scs2/22*Δ cells with and without Mdm36 overexpression. Each image is a maximum intensity projection of five optical sections spaced 0.5 µm apart. Plot showing mean fluorescence intensity of individual Num1-GFP patches in indicated strains. Error bar represents SEM. *P*-value by one-way ANOVA test.

Journal of Cell Science • Supplementary information

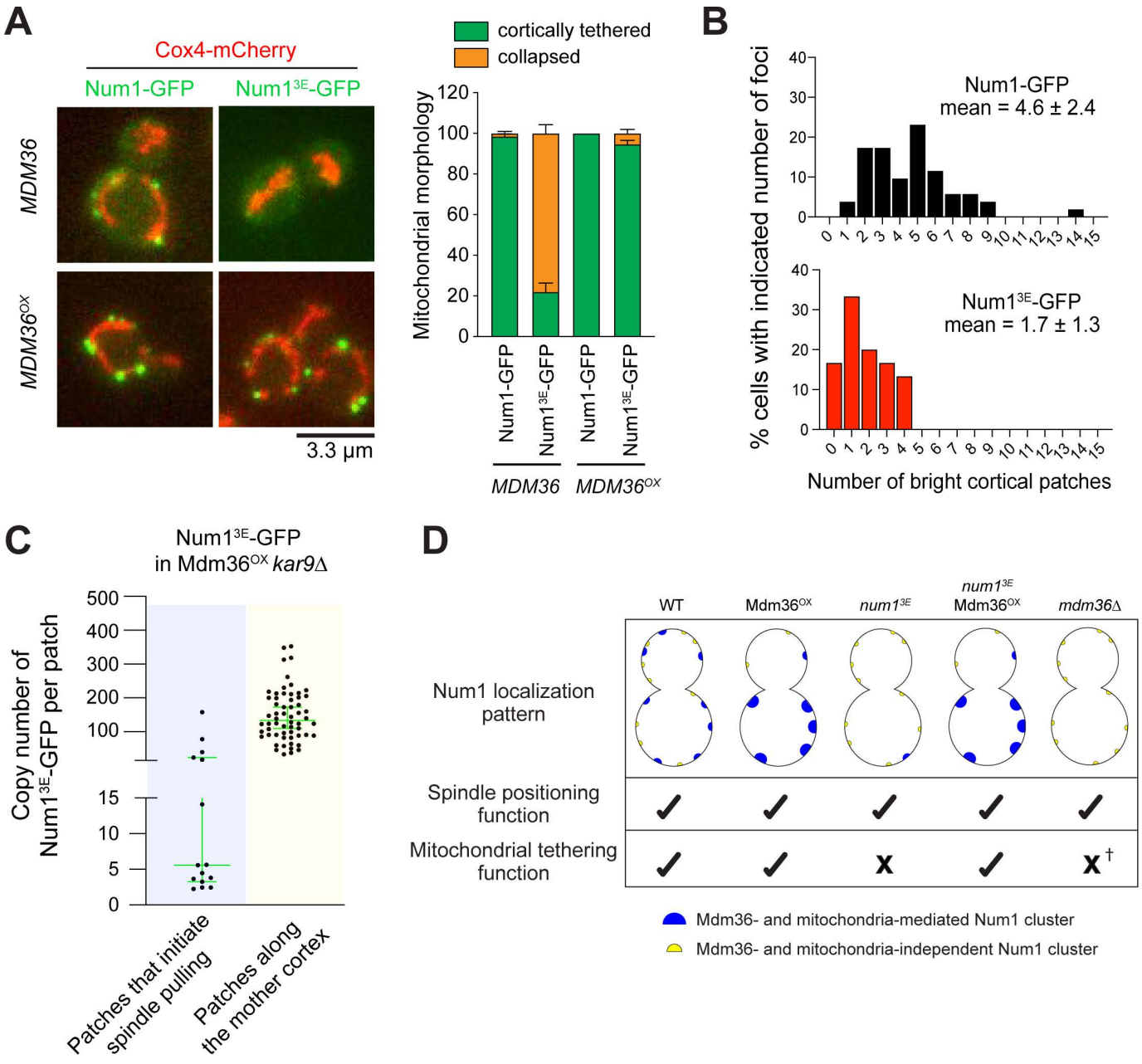

Figure S3. 3E mutations disrupt mitochondrial tethering but not spindle positioning function of Num1. (A) Wide-field images of Cox4-mCherry cells expressing Num1-GFP and Num1^{3E}-GFP with and without Mdm36 overexpression. *Right*, quantification of mitochondrial morphology in indicated strains. Mitochondrial network is considered collapsed if the network

Journal of Cell Science • Supplementary information

fails to show tubular morphology and appears meshed or aggregated over the course of a 4-min movie. Error bars represent SEP. 91 ≤ n ≤ 131 cells per strain. (B) Percentage of Num1-GFP and Num1^{3E}-GFP cells with indicated number of cortical patches (30 ≤ n ≤ 52 cells). Mean number per cell ± SD is indicated. (C) Copy number of Num1^{3E}-GFP at individual cortical patches found along the mother cell cortex compared to those found in the bud cortex mediating spindle pulling during a spindle correction assay in Mdm36^{OX} *kar9*Δ cells (n = 60 and 15 patches, respectively). Median ± 95% confidence interval is indicated. (D) Graphical summary of Num1 localization pattern and the resultant spindle positioning and mitochondrial tethering function in the indicated strain backgrounds. †, based on mitochondrial phenotype of *mdm36*Δ (Hammermeister et al., 2010).

Journal of Cell Science • Supplementary information

Table S1. Yeast strains used in this study

Strain	Genotype	Source
YWL706	*MATα NUM1-yEGFP::spHIS5 ura3-52 lys2-801 leu2-Δ1 his3-Δ200 trp1-Δ63*	Omer et al., 2018
YWL4774	*MATa NUM1-yEGFP::spHIS5 HIS3p:mRuby2-TUB1+3'UTR::HPH^{R} ura3-52 lys2-801 leu2-Δ1 his3-Δ200 trp1-Δ63*	Omer et al., 2018
YWL4959	*MATα num1$^{L167E+L170E}$-yEGFP::spHIS5 HIS3p:mRuby2-TUB1+3'UTR::URA3 ura3-52 lys2-801 leu2-Δ1 his3-Δ200 trp1-Δ63*	Omer et al., 2018
YWL4966	*MATα NUM1-yEGFP::spHIS5 kar9Δ::KAN^{R} HIS3p:mRuby2-TUB1+3'UTR::URA3 ura3-52 lys2-801 leu2-Δ1 his3-Δ200 trp1-Δ63*	Omer et al., 2018
YWL5664	*MATα NUM1-yEGFP::spHIS5 HPH^{R}::MET3p:MDM36 ura3-52 lys2-801 leu2-Δ1 his3-Δ200 trp1-Δ63*	This study
YWL4792	*MATa mdm36Δ::KAN^{R} NUM1-yEGFP::spHIS5 ura3-52 lys2-801 leu2-Δ1 his3-Δ200 trp1-Δ63*	This study
YWL4879	*MATa mdm36Δ::KAN^{R} NUM1-yEGFP::spHIS5 HIS3p:mRuby2-TUB1+3'UTR::URA3 ura3-52 lys2-801 leu2-Δ1 his3-Δ200 trp1-Δ63*	This study
YWL5685	*MATα NUM1-yEGFP::spHIS5 HPH^{R}::MET3p:MDM36 HIS3p:mRuby2-TUB1+3'UTR::URA3 ura3-52 lys2-801 leu2-Δ1 his3-Δ200 trp1-Δ63*	This study
YWL4135	*MATα DYN1-3GFP::TRP1 mCherry-TUB1::LEU2 ura3-52 lys2-801 leu2-Δ1 his3-Δ200 trp1-Δ63*	This study
YWL5682	*MATα DYN1-3GFP::TRP1 HPH^{R}::MET3p:MDM36 HIS3p:mRuby2-TUB1+3'UTR::URA3 ura3-52 lys2-801 leu2-Δ1 his3-Δ200 trp1-Δ63*	This study
YWL2076	*MATα JNM1-3mCherry::HIS3 GFP-TUB1::LEU2 ura3-52 lys2-801 leu2-Δ1 his3-Δ200 trp1-Δ63*	Tang et al., 2012
YWL5673	*MATα JNM1-3mCherry::HIS3 GFP-TUB1::LEU2 HPH^{R}::MET3p:MDM36 ura3-52 lys2-801 leu2-Δ1 his3-Δ200 trp1-Δ63*	This study
YWL5685	*MATα NUM1-yEGFP::spHIS5 HPH^{R}::MET3p:MDM36 HIS3p:mRuby2-TUB1+3'UTR::URA3 ura3-52 lys2-801 leu2-Δ1 his3-Δ200 trp1-Δ63*	This study
YWL4959	*MATα num1$^{L167E+L170E}$-yEGFP::spHIS5 HIS3p:mRuby2-TUB1+3'UTR::URA3 ura3-52 lys2-801 leu2-Δ1 his3-Δ200 trp1-Δ63*	Omer et al., 2018
YWL5694	*MATa num1$^{L167E+L170E}$-yEGFP::spHIS5 HPH^{R}::MET3p:MDM36 HIS3p:mRuby2-TUB1+3'UTR::URA3 ura3-52 lys2-801 leu2-Δ1 his3-Δ200 trp1-Δ63*	This study
YWL4966	*MATα NUM1-yEGFP::spHIS5 kar9Δ::KAN^{R} HIS3p:mRuby2-TUB1+3'UTR::URA3 ura3-52 lys2-801 leu2-Δ1 his3-Δ200 trp1-Δ63*	Omer et al., 2018
YWL5667	*MATα NUM1-yEGFP::spHIS5 kar9Δ::KAN^{R} HPH^{R}::MET3p:MDM36 HIS3p:mRuby2-*	This study

	TUB1+3'UTR::URA3 ura3-52 lys2-801 leu2-Δ1 his3-Δ200 trp1-Δ63	
YWL5724	*MATa num1$^{K121E+R262E+R265E}$-yEGFP::spHIS5 ura3-52 lys2-801 leu2-Δ1 his3-Δ200 trp1-Δ63*	This study
YWL2572	*MATα NUM1-yEGFP::spHIS5 COX4-mCherry::URA3 ura3-52 lys2-801 leu2-Δ1 his3-Δ200 trp1-Δ63*	Omer et al., 2018
YWL5740	*MATa num1$^{K121E+R262E+R265E}$-yEGFP::spHIS5 COX4-mCherry::URA3 ura3-52 lys2-801 leu2-Δ1 his3-Δ200 trp1-Δ63*	This study
YWL5760	*MATa num1$^{K121E+R262E+R265E}$-yEGFP::spHIS5 COX4-mCherry::URA3 HPH^{R}::MET3p:MDM36 ura3-52 lys2-801 leu2-Δ1 his3-Δ200 trp1-Δ63*	This study
YWL488	*MATa kar9Δ::TRP1 ura3-52 lys2-801 leu2-Δ1 his3-Δ200 trp1-Δ63*	This study
YWL484	*MATα kar9Δ::TRP1 ura3-52 lys2-801 leu2-Δ1 his3-Δ200 trp1-Δ63*	Tang et al., 2009
YWL3784	*MATa num1$^{L167E+L170E}$::LEU2 ura3-52 lys2-801 leu2-Δ1 his3-Δ200 trp1-Δ63*	This study
YWL5659	*MATα mdm36Δ::KAN^{R} ura3-52 lys2-801 leu2-Δ1 his3-Δ200 trp1-Δ63*	This study
YWL5656	*MATa kar9Δ::TRP1 ura3-52 lys2-801 leu2-Δ1 his3-Δ200 trp1-Δ63*	This study
YWL5670	*MATα HPH^{R}::MET3p:MDM36 ura3-52 lys2-801 leu2-Δ1 his3-Δ200 trp1-Δ63*	This study
YWL5671	*MATa HPH^{R}::MET3p:MDM36 ura3-52 lys2-801 leu2-Δ1 his3-Δ200 trp1-Δ63*	This study
YWL5715	*MATa NUM1-yEGFP::spHIS5 COX4-mCherry::URA3 HPH^{R}::MET3p:MDM36 ura3-52 lys2-801 leu2-Δ1 his3-Δ200 trp1-Δ63*	This study
YWL5714	*MATa NUM1-yEGFP::spHIS5 COX4-mCherry::URA3 HPH^{R}::MET3p:MDM36 ura3-52 lys2-801 leu2-Δ1 his3-Δ200 trp1-Δ63*	This study
YWL4834	*MATa NUM1-yEGFP::spHIS5 mdm36Δ::KAN^{R} COX4-mCherry::URA3 ura3-52 lys2-801 leu2-Δ1 his3-Δ200 trp1-Δ63*	This study
YWL5737	*MATa num1$^{K121E+R262E+R265E}$-yEGFP::spHIS5 HIS3p:mRuby2-TUB1+3'UTR::URA3 ura3-52 lys2-801 leu2-Δ1 his3-Δ200 trp1-Δ63*	This study
YWL5763	*MATa num1$^{K121E+R262E+R265E}$-yEGFP::spHIS5 HIS3p:mRuby2-TUB1+3'UTR::URA3 kar9Δ::TRP1 ura3-52 lys2-801 leu2-Δ1 his3-Δ200 trp1-Δ63*	This study
YWL5758	*MATa num1$^{K121E+R262E+R265E}$-yEGFP::spHIS5 HIS3p:mRuby2-TUB1+3'UTR::URA3 HPH^{R}::MET3p:MDM36 ura3-52 lys2-801 leu2-Δ1 his3-Δ200 trp1-Δ63*	This study
YWL5765	*MATa num1$^{K121E+R262E+R265E}$-yEGFP::spHIS5 HIS3p:mRuby2-TUB1+3'UTR::URA3 HPH^{R}::MET3p:MDM36 kar9Δ::TRP1 ura3-52 lys2-801 leu2-Δ1 his3-Δ200 trp1-Δ63*	This study

YWL3955	*MATa cin8Δ::spHIS5 GFP-TUB1::LEU2 ura3-52 lys2-801 leu2-Δ1 his3-Δ200 trp1-Δ63*	Omer et al., 2018
YWL5670	*MATα HPH^{R}::MET3p:MDM36 ura3-52 lys2-801 leu2-Δ1 his3-Δ200 trp1-Δ63*	This study
YWL5722	*MATα HPH^{R}::MET3p:NUM1-yEGFP::spHIS5 COX4-mCherry::URA3 ura3-52 lys2-801 leu2-Δ1 his3-Δ200 trp1-Δ63*	This study
YWL4764	*MATa NUM1-yEGFP::spHIS5 scs2Δ::TRP1 scs22Δ::KAN^{R} ura3-52 lys2-801 leu2-Δ1 his3-Δ200 trp1-Δ63*	Omer et al., 2018
YWL5984	*MATa NUM1-yEGFP::spHIS5 scs2Δ::TRP1 scs22Δ::KAN^{R} HPH^{R}::MET3p:MDM36 ura3-52 lys2-801 leu2-Δ1 his3-Δ200 trp1-Δ63*	This study
YWL6002	*MATa NUM1-yEGFP::spHIS5 COX4-mCherry::URA3 kar9Δ::TRP1 HPH^{R}::MET3p:MDM36 HIS3p:Venus-TUB1+3'UTR::LEU2 ura3-52 lys2-801 leu2-Δ1 his3-Δ200 trp1-Δ63*	This study
YWL1124	*MATα CSE4-yEGFP::spHIS5 ura3-52 lys2-801 leu2-Δ1 his3-Δ200 trp1-Δ63*	This study
YWL6058	*MATα NUM1-yEGFP::spHIS5 kar9Δ::KAN^{R} MET3p:mRuby2-MDM36::LEU2 HIS3p:Venus-TUB1+3'UTR::TRP1 ura3-52 lys2-801 leu2-Δ1 his3-Δ200 trp1-Δ63*	This study
YWL6056	*MATα NUM1-yEGFP::spHIS5 kar9Δ::KAN^{R} MET3p:mRuby2-MDM36::LEU2 HIS3p:Venus-TUB1+3'UTR::TRP1 ura3-52 lys2-801 leu2-Δ1 his3-Δ200 trp1-Δ63*	This study
YWL5767	*MATa NUM1-mRuby3::KAN^{R} HPH^{R}::MET3p:MDM36 DYN1-3GFP::TRP1 ura3-52 lys2-801 leu2-Δ1 his3-Δ200 trp1-Δ63*	This study
YWL5225	*MATa NUM1-yEGFP::spHIS5 mdm36Δ::KAN^{R} COX4-mCherry::URA3 MET3p:MDM36::LEU2 ura3-52 lys2-801 leu2-Δ1 his3-Δ200 trp1-Δ63*	This study
YWL5796	*MATα DYN1-3GFP::TRP1 COX4-mCherry::URA3 HPH^{R}::MET3p:MDM36 ura3-52 lys2-801 leu2-Δ1 his3-Δ200 trp1-Δ63*	This study
YWL4879	*MATa mdm36Δ::KAN^{R} NUM1-yEGFP::spHIS5 HIS3p:mRuby2-TUB1+3'UTR::URA3 ura3-52 lys2-801 leu2-Δ1 his3-Δ200 trp1-Δ63*	This study
YWL5473	*MATa mdm36Δ::KAN^{R} kar9Δ::TRP1 NUM1-yEGFP::spHIS5 HIS3p:mRuby2-TUB1+3'UTR::URA3 ura3-52 lys2-801 leu2-Δ1 his3-Δ200 trp1-Δ63*	This study
YWL6127	*MATα DYN1-3GFP::TRP1 num1$^{L167E+L170E}$::LEU2 HPH^{R}::MET3p:MDM36 HIS3p:mRuby2-TUB1+3'UTR::URA3 ura3-52 lys2-801 leu2-Δ1 his3-Δ200 trp1-Δ63*	This study
YWL6128	*MATa MIF2-yEGFP::spHIS5 ura3-52 lys2-801 leu2-Δ1 his3-Δ200 trp1-Δ63*	This study

Movie 1. Enhanced Num1 patches in Mdm36^{OX} cells are stationary and remarkably stable. Time-lapse images of Num1-GFP in a Mdm36^{OX} cell showing enhanced Num1 patches persisting for greater than two cell division cycles. Each frame is a maximum intensity projection of 9 optical sections spaced 0.5 µm apart. Movie captured at 10 min intervals.

Journal of Cell Science • Supplementary information

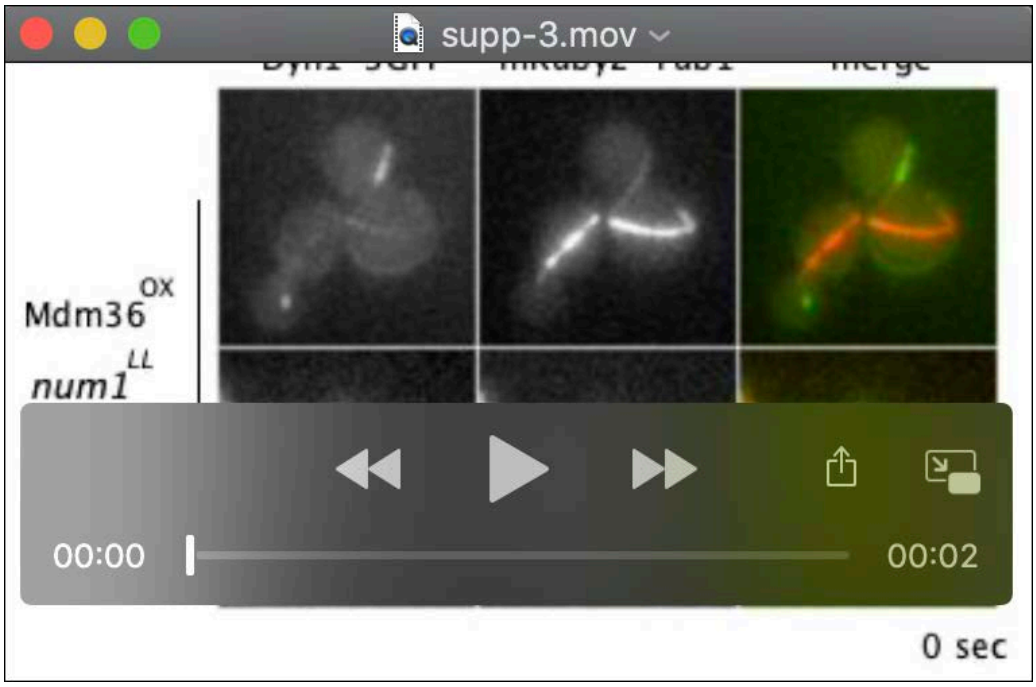

Movie 2. Num1^{LL} abolishes cortical localization of Dyn1-3GFP in Mdm36^{OX} cells. Time-lapse images of Dyn1-3GFP in Mdm36^{OX} cells expressing mRuby2-Tub1 showing accumulation of dynein at the MT plus ends. No stationary cortical Dyn1-3GFP foci were observed. Each frame is a maximum intensity projection of 5 wide-field sections spaced 0.5 µm apart. Movie captured at 10 s intervals.

Journal of Cell Science • Supplementary information

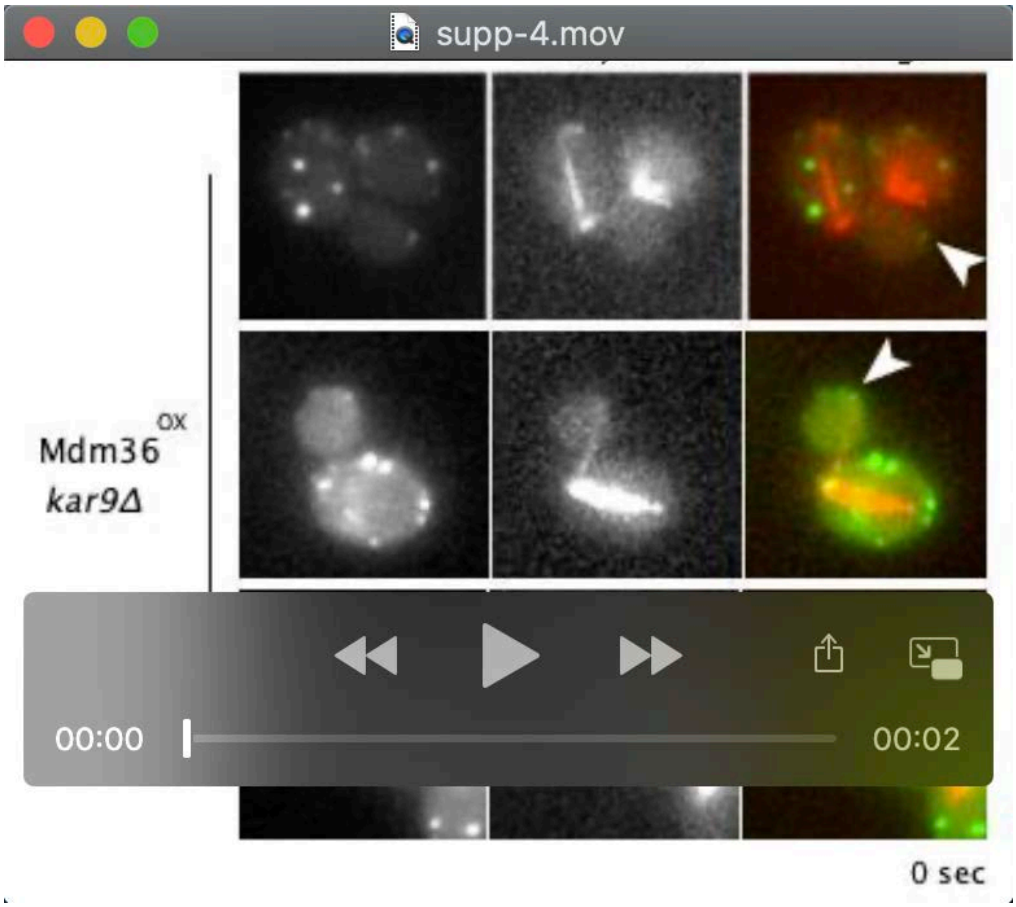

Movie 3. MT sliding initiates at a dim Num1 patch. Time-lapse images of Num1-GFP and mRuby2-Tub1 in Mdm36^{OX} *kar9*Δ cells showing examples of MT sliding events initiated by the plus end contacting a dim Num1 patch (arrowheads) at the bud cortex, followed by spindle correction. Each frame is a maximum intensity projection of 5 wide-field sections spaced 0.5 µm apart. Movie captured at 10 s intervals.

Journal of Cell Science • Supplementary information

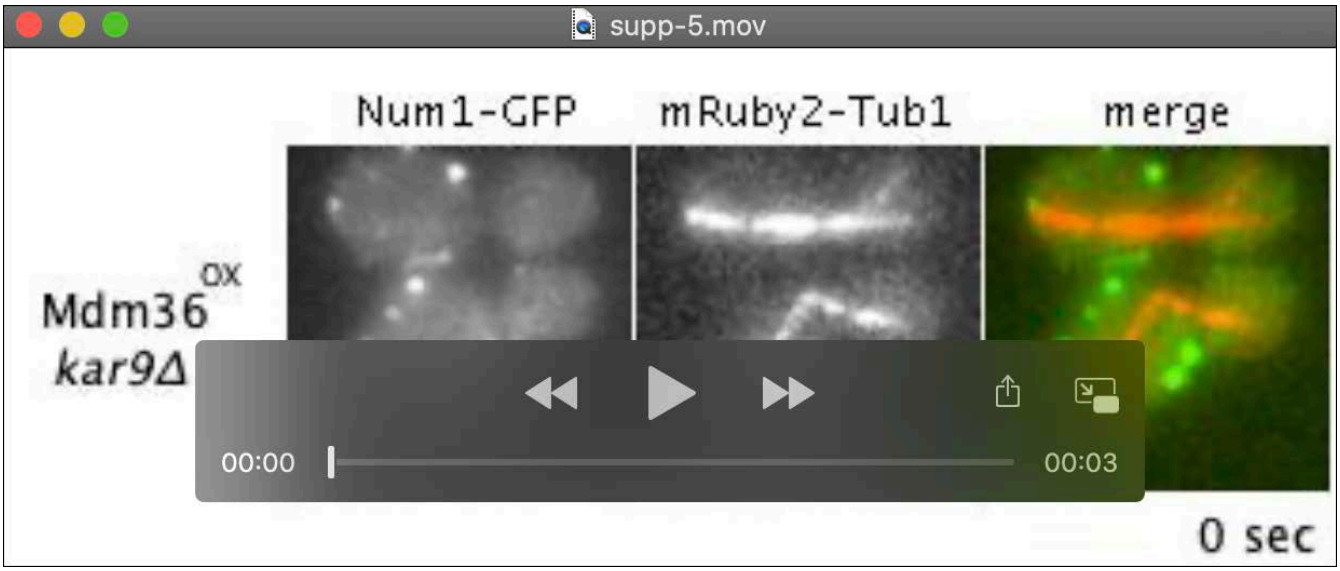

Movie 4. MT sliding occurring at a bud cortical region without visible Num1-GFP. Time-lapse images of Num1-GFP and mRuby2-Tub1 in Mdm36^{OX} *kar9*Δ cells. Frames from 60 s to 80 s and from 130 s to 150 s show MT sliding along the bud cortex (arrows) for the bottom and top cells, respectively. Each frame is a maximum intensity projection of 5 wide-field images spaced 0.5 µm apart. Movie captured at 10 s intervals.

Journal of Cell Science • Supplementary information

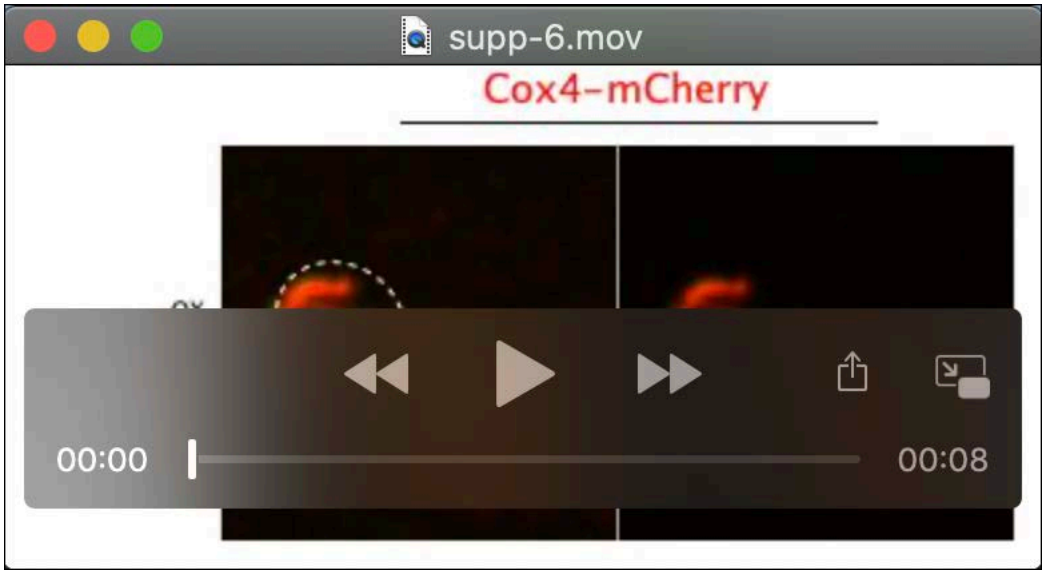

Movie 5. Mdm36^{OX} cells display branched and tubular mitochondrial network. Full 3D reconstruction of a deconvolved wide-field image stack showing a cell expressing Num1-GFP and mitochondria-targeted Cox4-mCherry in the Mdm36^{OX} background. Image stack consists of 11 optical sections spaced 0.5 µm apart.

Journal of Cell Science • Supplementary information

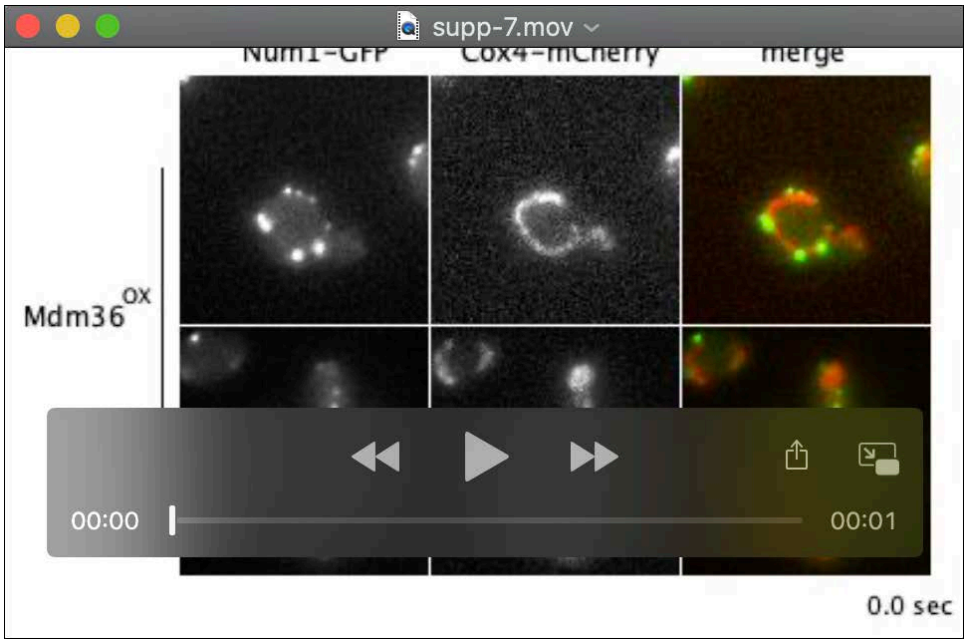

Movie 6. Mdm36^{ox} cells exhibit a persistent mitochondrial tethering phenotype. Time-lapse images of Num1-GFP and Cox4-mCherry in Mdm36^{OX} cells showing persistent tethering of mitochondria at the brightly enhanced cortical Num1 patches. Each frame is a maximum intensity projection of 5 wide-field sections spaced 0.5 µm apart. Movie captured at 17.5 s intervals.

Journal of Cell Science • Supplementary information

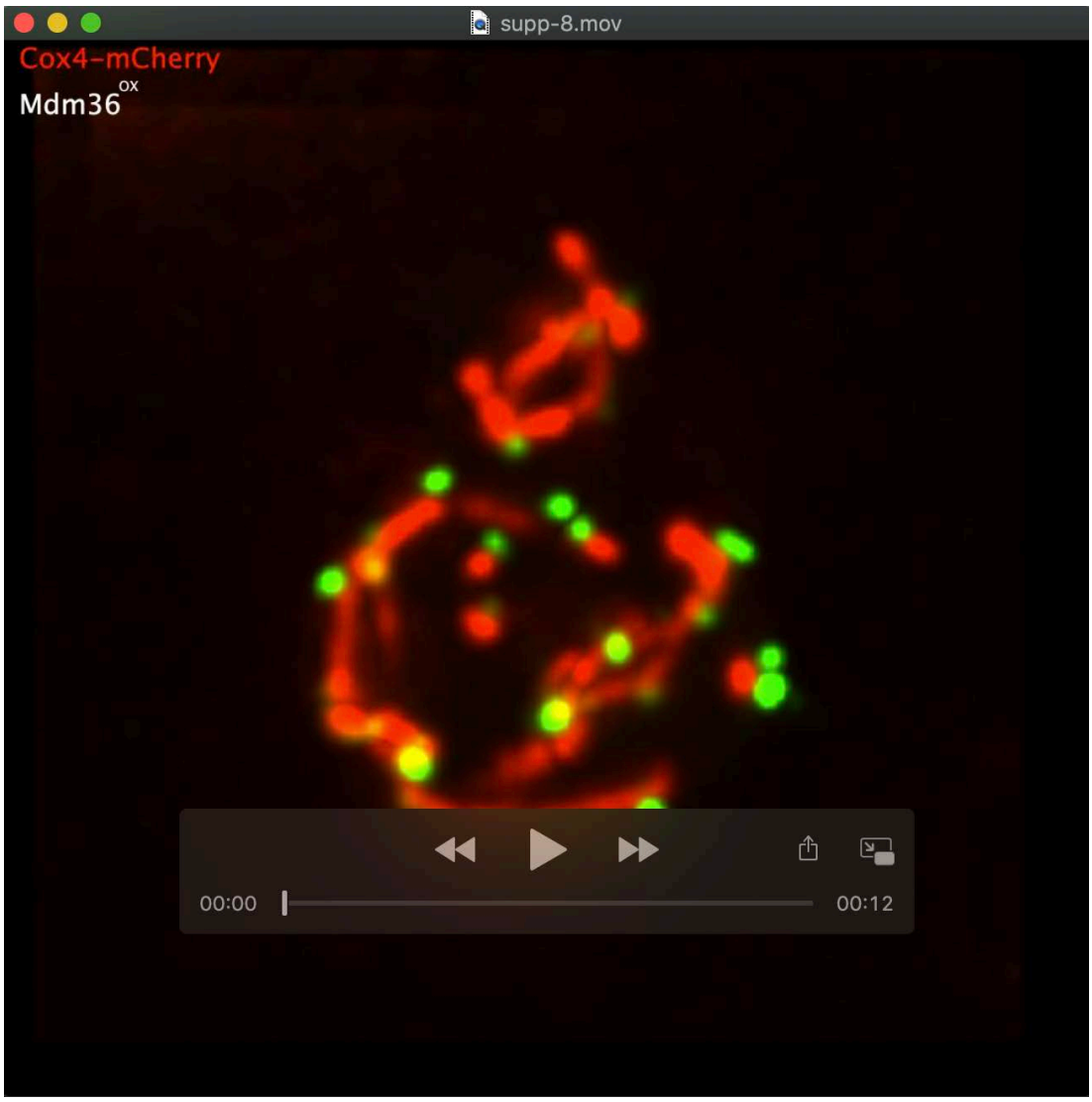

Movie 7. Mitochondrial network is tethered by enhanced Num1 foci in Mdm36^{ox} cells. Full 3D reconstruction of a deconvolved wide-field image stack showing mitochondria association with every single enhanced Num1-GFP patches in a Mdm36^{OX} cell. Mdm36 was overexpressed using a *MET3p:MDM36* plasmid integrated at the *leu2* locus. Image stack consists of 31 optical sections spaced 0.2 µm apart encompassing the entire thickness of the cell.

Journal of Cell Science • Supplementary information

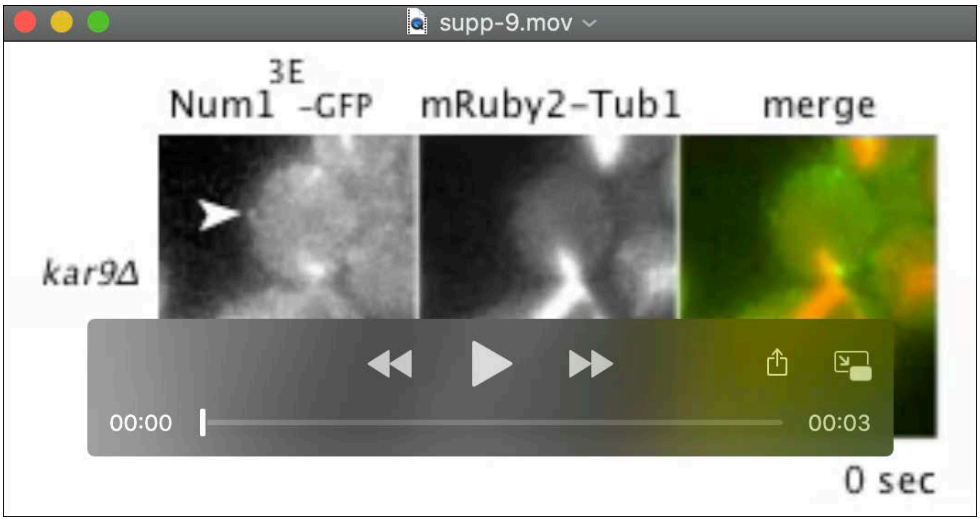

Movie 8. MT sliding initiates at a dim Num1^{3E} patch. Time-lapse images of Num1^{3E}-GFP and mRuby2-Tub1 in a *kar9*Δ cell. Frames at 0 s through 80 s show a dim cortical Num1^{3E}-GFP patch (arrowhead) that photobleached in later frames. Frame at 130 s shows the plus end contacting the site of the dim Num1^{3E}-GFP patch, followed by MT sliding in the subsequent frame. Each frame is a maximum intensity projection of 5 wide-field sections spaced 0.5 µm apart. Movie captured at 10 s intervals.

Journal of Cell Science • Supplementary information